Inorganic Chemistry

Article

pubs.acs.org/IC

Tandem Postsynthetic Metal Ion and Ligand Exchange in Zeolitic Imidazolate Frameworks

Honghan Fei,[†] John F. Cahill,[†] Kimberly A. Prather,[†,‡] and Seth M. Cohen*[,†]

[†]Department of Chemistry and Biochemistry and [‡]Scripps Institute of Oceanography, University of California, San Diego, La Jolla, California 92093, United States

Supporting Information

ABSTRACT: Herein, we report a general postsynthetic exchange (PSE) approach to introduce a redox-active transition metal, specifically Mn(II), into "inert" zeolitic imidazolate frameworks (ZIFs), a subclass of metal–organic frameworks (MOFs). It is shown that metal ion PSE occurs in ZIF-71 (**RHO** topology) and ZIF-8 (**SOD** topology) under ambient conditions. The metal exchanged ZIFs are the first porous, Mn(II)-based ZIFs and a rare example of ZIFs with two transition metal centers in a single lattice. Exchanged materials are characterized by scanning electron microscopy-energy dispersed X-ray spectroscopy (SEM-EDX), aerosol time-of-flight mass spectrometry (ATOFMS), X-ray fluorescence spectroscopy (XRF), and Brunauer–Emmett–Teller (BET) surface area analysis. In addition, stepwise "tandem" PSE strategies are described to exchange of metal ions and organic linkers consecutively in ZIFs. These findings are important for probing the chemical dynamics of ZIFs, despite their high crystallinity and robustness, and inspire the more widespread use of PSE to prepare multimetallic and multifunctional MOFs.

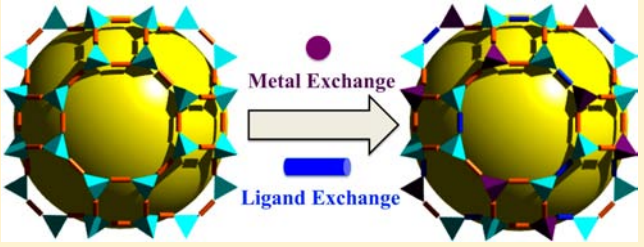

INTRODUCTION

Metal–organic frameworks (MOFs) are an emerging class of microporous materials with exponential growth in recent years not only because of their vast array of topologies with metal-based building blocks and organic linkers[1] but also because of their applications in gas absorption/separation,[2,3] catalysis,[4] and chemical separations.[5] Organic ligand components of MOFs allow for a great variety of functional groups, introduced by direct synthesis[6] or postsynthetic approaches, such as postsynthetic modification (PSM)[7−9] and postsynthetic deprotection (PSD).[10−13]

Recently, postsynthetic exchange (PSE) of MOFs has been discovered via the metathesis of organic linkers, as well as metal ions in the secondary-building units of MOFs (SBUs), while retaining structural integrity and high porosity.[14−19] The relatively mild conditions are effective for introducing new metal ions and functionalized ligands that cannot be introduced by direct solvothermal synthesis. However, many reports of this exchange strategy focus on less stable MOFs with more labile metal–ligand bonding. Most of the technological applications proposed for MOFs would require highly robust materials, especially with respect to water and air.[20,21] Incredibly, PSE has also been observed in these "inert" MOFs,[22−25] which are considered to be robust with enhanced thermal and chemical stability, such as UiO (University of Oslo) materials,[26] MIL (Materials Institute Lavoiser) materials,[27] and ZIFs (Zeolitic Imidazolate Frameworks).[28] Metal ion and/or ligand PSE were observed in solvent-mediated solid–solid reactions, as well as under solid–liquid conditions. Indeed, PSE is becoming increasingly established as a promising approach to post-synthetically functionalize a variety of MOFs. Importantly, PSE provides insight into the underlying chemical dynamics between SBUs and organic linkers in even highly robust MOFs.

ZIFs, mostly based on Zn(II) and Co(II), are recognized as a subclass of highly robust MOFs combining inorganic zeotype topologies and organic functionalities.[28−30] Their exceptionally high chemical and thermal robustness were widely recognized as evidenced by their stability in boiling, basic solutions.[29] Very recently, Hupp and co-workers reported solvent-assisted ligand exchange (SALE) on ZIFs,[31] and some of the resulting 'SALEM' materials displayed Brønsted basicity upon *n*-butyllithium treatment.[22] The application of PSE to produce mixed-metal (i.e., solid-solution) ZIFs has not been explored. Herein, we report metal ion PSE in ZIFs and introduce redox-active Mn(II) centers into porous Zn(II)-based ZIFs for the first time. ZIFs with two typical zeotype topologies, **RHO** and **SOD**, were chosen as initial examples for this metal-based PSE. In addition, stepwise "tandem" PSE strategies are described with exchange of both metal ions and organic ligands consecutively on ZIFs. These findings are important to illustrate PSE as a general route for preparing bimetallic and multifunctional MOFs that retain their parent topology.

EXPERIMENTAL METHODS

General Methods. Starting materials and solvents were purchased and used without further purification from comercial suppliers (Aldrich, Sigma-Aldrich, Alfa Aesar, EMD, TCI, Cambridge Isotope

Received: January 8, 2013
Published: March 21, 2013

   dx.doi.org/10.1021/ic400048g | *Inorg. Chem.* 2013, 52, 4011−4016

Laboratories, Inc., and others). Proton nuclear magnetic resonance spectra (^{1}H NMR) were recorded on a Varian FT-NMR spectrometer (400 MHz for ^{1}H NMR). Chemical shifts were quoted in parts per million (ppm) referenced to the appropriate solvent peak or 0 ppm for TMS. ZIF-71(Zn) and ZIF-8(Zn) were prepared and activated as previously described.[32,33]

Solid−Liquid PSE between ZIF and Mn(II). $Mn(acac)_2$ (0.6 mmol, 150 mg) was dissolved in MeOH (5 mL). This solution was added to ZIF(Zn) (ca. 67 mg, 0.2 mmol equiv. of Zn for ZIF-71; ca. 45 mg, 0.2 mmol equiv. of Zn for ZIF-8), and the mixture was incubated at 55 °C in a preheated oven for 24 h. After cooling, the mixture was centrifuged and the solvent decanted. The solids were washed with 2 × 10 mL of MeOH or until supernatant was colorless. The solids were left to soak in MeOH for 3 d, and the solution was exchanged with fresh MeOH (10 mL) every 24 h. After 3 d of soaking, the solids were centrifuged and dried at 75 °C in air.

Comparison Experiment of ZIF(Zn/Mn) Before Washing. $Mn(acac)_2$ (0.6 mmol, 150 mg) was dissolved in MeOH (5 mL). This solution was added to ZIF(Zn) (ca. 67 mg, 0.2 mmol equiv. of Zn for ZIF-71; ca. 45 mg, 0.2 mmol equiv. of Zn for ZIF-8), and mixture was incubated at 55 °C in a preheated oven for 24 h. After cooling, the mixture was centrifuged and the solvent decanted. The solids were directly dried at 75 °C in air.

Stepwise PSE of ZIF via Strategy I. 4-Bromo-1*H*-imidazole (87 mg, 0.6 mmol) was dissolved in MeOH (5 mL). This solution was added to ZIF(Zn) (ca. 34 mg, 0.2 mmol equiv. of 4,5-dichloroimidazolate for ZIF-71; ca. 23 mg, 0.2 mmol equiv. of 2-methylimidazolate for ZIF-8), and the mixture was incubated at 55 °C in a preheated oven for 3 d. After cooling, the mixture was centrifuged and the solids washed with 3 × 10 mL of MeOH. The solids were left to soak in MeOH for 3 d, and the solution was exchanged with fresh MeOH (10 mL) every 24 h. After 3 d of soaking, the solids were centrifuged and dried at 75 °C in air.

Dried ligand-exchanged ZIF solids (ca. 68 mg, 0.2 mmol equiv. of Zn for ZIF-71; ca. 53 mg, 0.2 mmol equiv. of Zn for ZIF-8) were introduced into a MeOH (5 mL) solution containing $Mn(acac)_2$ (0.6 mmol, 150 mg). The mixture was incubated at 55 °C in a preheated oven for 24 h. After cooling, the mixture was centrifuged and washed with 2 × 10 mL of MeOH or until supernatant was colorless. The solids were left to soak in MeOH for 3 d, and the solution was exchanged with fresh MeOH (10 mL) every 24 h. After 3 d of soaking, the solids were centrifuged and dried at 75 °C in air.

Stepwise PSE of ZIF via Strategy II. 4-Bromo-1*H*-imidazole (87 mg, 0.6 mmol) was dissolved in MeOH (5 mL). This solution was added to dried solids after solid−liquid PSE with Mn(II) (ca. 34 mg, 0.2 mmol equiv. of 4,5-dichloroimidazolate for ZIF-71(Zn/Mn); ca. 23 mg, 0.2 mmol equiv. of 2-methylimidazolate for ZIF-8(Zn/Mn)), and the mixture was incubated at 55 °C in a preheated oven for 3 d. After cooling, the mixture was centrifuged and washed with 3 × 10 mL of MeOH. The solids were left to soak in MeOH for 3 d, and the solution was exchanged with fresh MeOH (10 mL) every 24 h. After 3 d of soaking, the solids were centrifuged and dried at 75 °C in air.

Direct Synthesis of ZIF-71(Zn/Mn). A solution of zinc acetate (132 mg, 0.72 mmol), $Mn(OAc)_2{\cdot}4H_2O$ (14 mg, 0.08 mmol) in 8 mL of *N*,*N*-dimethylformamide and a solution of 4,5-dichloroimidazole (329 mg, 2.4 mmol) in 8 mL *N*,*N*-dimethylformamide were combined and sealed in a 20 mL vial, and heated in a preheated oven at 85 °C for 12 h. After cooling, the mother liquor was decanted and the solids were washed with chloroform (3 × 10 mL). Then the solids were left to soak in chloroform for 3 d, and the solution was exchanged with fresh chloroform (10 mL) every 24 h. After 3 d of soaking, the solids were centrifuged and dried at 80 °C under vacuum.

Direct Synthesis of ZIF-8(Zn/Mn). A solid mixture of $Zn(NO_3)_2{\cdot}6H_2O$ (215 mg, 0.73 mmol), Mn(II) (0.07 mmol, 17.2 mg for $Mn(OAc)_2{\cdot}4H_2O$; 17.7 mg for $Mn(acac)_2$; 13.9 mg for $MnCl_2{\cdot}4H_2O$), and 2-methyl-imidazole (60 mg, 0.73 mmol) were dissolved in DMF (18 mL). This solution was capped and sealed in a 20 mL vial, and heated to 140 °C for 24 h. After cooling, the mother liquor was decanted, and the solids were washed with chloroform (3 × 10 mL). The solids were left to soak in chloroform for 3 d, and the solution was exchanged with fresh chloroform (10 mL) every 24 h. After 3 d of soaking, the solids were centrifuged and dried under vacuum.

PXRD Analysis. Approximately 20−30 mg of ZIF material was dried at 75 °C prior to PXRD analysis. PXRD data were collected at ambient temperature on a Bruker D8 Advance diffractometer at 40 kV, 40 mA for Cu Kα (λ = 1.5418 Å), with a scan speed of 1 s/step, a step size of 0.02° in 2θ, and a 2θ range of 3−45° (sample dependent). The experimental backgrounds were corrected using the Jade 5.0 software package.

Digestion and Analysis by ^{1}H NMR. Approximately 10 mg of ZIF material was dried under vacuum at 75 °C and digested with sonication in 575 μL of MeOH-d_4 and 25 μL of 35% DCl in D_2O.

Brunauer−Emmett−Teller (BET) Surface Area Analysis. Approximately 50 mg of ZIF material was evacuated on a vacuum line for 2 h at room temperature. The sample was then transferred to a preweighed sample tube and degassed at 105 °C on an Micromeritics ASAP 2020 Adsorption Analyzer for a minimum of 12 h or until the outgas rate was <5 mm Hg. The sample tube was reweighed to obtain a consistent mass for the degassed exchanged MOF. BET surface area (m^2/g) measurements were collected at 77 K by N_2 on a Micromeritics ASAP 2020 Adsorption Analyzer using the volumetric technique.

Thermogravimetric Analysis. Approximately 10−15 mg of ZIF material after BET analysis (activated) was used for TGA measurements. Samples were analyzed under N_2 stream using a TA Instruments Q600 SDT running from room temperature to 800 °C with a scan rate of 5 °C/min.

Scanning Electron Microscopy-Energy Dispersed X-ray Spectroscopy. Approximately 2−5 mg of activated ZIF material was transferred to conductive carbon tape on a sample holder disk. A Philips XL ESEM instrument was used for acquiring images using a 10−20 kV energy source under vacuum. Oxford EDX and Inca software were used for elemental mapping of particle surfaces at a working distance at 10 mm. Images were collected at a magnification of ∼10000×.

Digestion and Analysis by X-ray Fluorescence. Approximately 30−50 mg of activated ZIF material was digested with sonication in 1 M HCl (3 mL). The digested samples were analyzed using a Panalytical MiniPal4 Energy Dispersed X-ray Fluorescence Spectrometer.

Aerosol Time-of-Flight Mass Spectrometry (ATOFMS). Dry ZIF materials were aerosolized using flow of High-Efficiency Particulate Air (HEPA) filtered air. The particles were drawn into an aerosol time-of-flight mass spectrometer (ATOFMS) where they were accelerated to their terminal aerodynamic velocities.[34] Particles pass through two continuous-wave diode pumped 532 nm laser beams (Crystal Laser, Reno, NV) positioned 6 cm apart. The time difference between the light scattering signals is used to calculate the velocity of the particle. The aerodynamic diameter of the particle is calculated using particle velocities and a calibration curve created using known-size polystyrene latex spheres (PSL, Inviterogen, 0.2−3 μm in diameter). Particle velocities are also used to time the firing of a pulsed 266-nm Nd:YAG laser (Nd:YAG, Quantel, Newbury, UK) operating at ∼1 mJ (∼10^8 W/cm^2). The laser pulse desorbs and ionizes species from the particle, and the generated ions are detected using a dual polarity reflection time-of-flight mass spectrometer. The mass spectra of the positive and negative ions along with the individual particle size information are recorded for data analysis.

Metal ion exchange for ZIF-71(Zn) was identified by the presence of the ions Mn^+ (m/z +55) and Zn^+ (m/z +64/66/68) in the positive ion spectrum. Ligand exchange for ZIF-71 materials was identified by the presence of the ions Cl^- (m/z −35 and −37, indicating the 4,5-dichloroimidazolate ligand) and Br^- (m/z −79 and −81, indicating the 4-bromoimidazolate ligand) in the negative ion spectrum of the particle. Particles without either positive or negative ion spectra were removed from the data analysis for the ligand exchange experiments. Approximately 500−1000 particles were collected for each sample.

Dry Aerosol Generation. Approximately 100 mg of dry ZIF materials were placed in a 1 L volumetric flask. Aerosol was generated

by agitating the sample with HEPA filtered air. A constant 1.0 lpm was brought into the ATOFMS for aerosol analysis at ~8−12 Hz.

Hierarchical Clustering (HC) Analysis. Clustering is used to reduce the volume of data into a much more manageable size. HC analysis groups similar mass spectra into clusters. Clusters can be manually divided into more clusters if significant differences between spectra exist. Clusters were finalized once further divisions of clusters had no significant impact on the average spectrum (i.e., all spectra in the cluster were identical).

RESULTS AND DISCUSSION

ZIF-71(Zn) with a **RHO** topology was prepared and activated according to a previously reported procedure.[32] Activated ZIF-71(Zn) was incubated in a solution of $Mn(acac)_2$ (acac = acetylacetonate) in MeOH at 55 °C for 24 h (Scheme 1). The

Scheme 1. Postsynthetic Mn(II) Exchange of ZIF-71

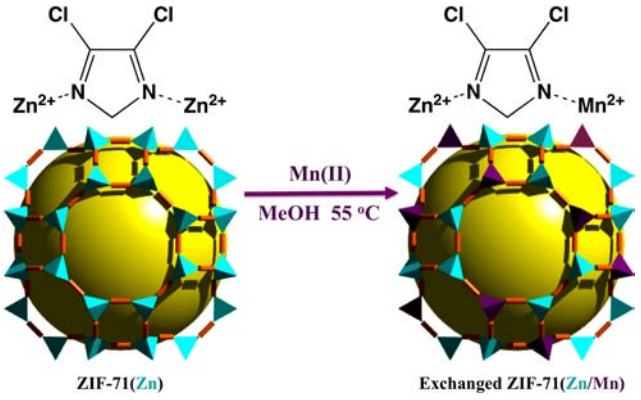

solids were isolated by centrifugation, washed with fresh MeOH, to give a pale brown microcrystalline powder. In addition to the observed color change, the presence of Mn(II) in ZIF-71 was confirmed by X-ray fluorescence spectroscopy (XRF), scanning electron microscopy-energy-dispersed X-ray spectroscopy (SEM-EDX), and aerosol time-of-flight mass spectrometry (ATOFMS).[34,35]

XRF analysis of pristine ZIF-71(Zn) confirmed negligible Mn (<0.05% by weight); however, exchanged ZIF-71(Zn/Mn) gave 2.3 ± 0.5% (by weight, Supporting Information, Table S1). As would be expected for a PSE process, the Zn content in exchanged ZIF-71(Zn/Mn) decreased from 20.2% (theoretical = 19.4%) to 16.7 ± 0.1%. These results indicate ~12% of the tetrahedral Zn(II) centers were exchanged for Mn(II). SEM-EDX of exchanged ZIF-71(Zn/Mn) exhibits signals of both Mn (Kα, 5888 eV) and Zn (Kα, 8616 eV), which gave an atomic ratio of Mn to Zn of 0.126:1, consistent with the XRF analysis (Supporting Information, Figure S1, Table S1). SEM-EDX mappings of exchanged ZIF-71(Zn/Mn) were measured to study the dispersity of Mn(II) in the exchanged products. SEM images clearly show identical particle size and morphology of ZIF-71 particles before and after exchange (Supporting Information, Figure S2, S3). Mn EDX mapping of exchanged ZIF-71(Zn/Mn) shows an identical distribution as Zn and Cl, which suggest the Mn ions are evenly spread throughout the particles. Finally, the positive ion ATOFMS spectra of exchanged ZIF-71(Zn/Mn) revealed both Zn (m/z = 64, 66, 68) and Mn (m/z = 55) in each particle, while only Zn ions were observed in parent ZIF-71(Zn) (Figure 1). Over 99% of the exchanged ZIF-71(Zn/Mn) particles (~1000 analyzed) contained both Zn and Mn ions, indicating that PSE occurred

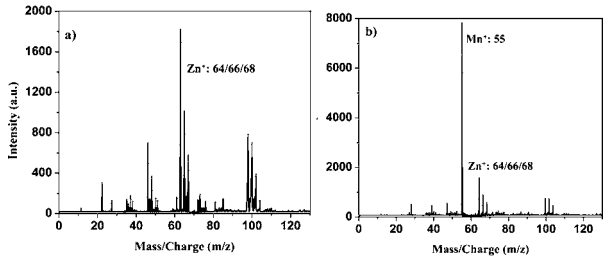

Figure 1. ATOFMS positive ion spectra of: (a) ZIF-71(Zn) and (b) exchanged ZIF-71(Zn/Mn).

in essentially all of the ZIF-71 particles. Exposing ZIF-71(Zn/Mn) to a 3 molar excess of $Zn(acac)_2$ in MeOH resulted in almost all of Mn(II) centers being exchanged back to Zn. EDX of the resulting material indicates a Zn:Mn atomic ratio of 99:1, compared with 7.3:1 prior to reintroduction of Zn(II). This suggests that this PSE process is under kinetic control.

Importantly, the highly porous **RHO** topology as well as the crystallinity of ZIF-71(Zn) were retained after PSE, as verified by powder X-ray diffraction (PXRD) (Supporting Information, Figure S4). BET surface areas of ZIFs before and after exchange were determined using N_2 (77 K) and show similar values for ZIF-71(Zn) (964 ± 9 m^2/g) and ZIF-71(Zn/Mn) (966 ± 12 m^2/g, Supporting Information, Table S3). Thermogravimetric analysis (TGA) of exchanged ZIF-71(Zn/Mn) also displayed nearly identical thermal stability (up to ~400 °C) and decomposition steps as ZIF-71(Zn) (Supporting Information, Figure S5). In addition to these results, we sought to provide evidence to rule out the possibility of free Mn ions or other Mn species residing in the pores of the ZIF. The ratio of metals in ZIF-71(Zn/Mn) that were activated, but not washed with MeOH, was determined to be 0.225:1 (Mn:Zn) via EDX (Supporting Information, Figure S6). The percentage of Mn(II) is 60% higher than that found after washing, verifying the importance of the washing step to remove loosely bound Mn(II) species in ZIF-71(Zn/Mn). Such included species would also be expected to change the gas sorption and/or thermal behavior of the ZIF. The BET surface area of activated, but unwashed ZIF-71(Zn/Mn), decreased to 854 m^2/g, and TGA showed a lower thermal stability and different decomposition steps (Supporting Information, Figure S5). In addition, XRF spectra of the $Mn(acac)_2$ solution before and after PSE were collected to monitor the exchange process. A release of 12.3% Zn(II) from ZIF-71(Zn) into the $Mn(acac)_2$ solution was observed upon completion of PSE. A concomitant 9.7% decrease in Mn(II) concentration was also detected, as expected. In summary, these experiments suggest no free Mn(II) ions, complexes, or particles reside in the MOF cages of fully washed and activated exchanged ZIF-71(Zn/Mn).

To investigate the generality of metal ion PSE with ZIFs, we employed another widely studied material, ZIF-8. Compared with ZIF-71, ZIF-8 possesses a different organic linker (2-methyl-imidazole in ZIF-8 versus 4,5-dichloro-imidazole in ZIF-71) and a different net topology (**SOD** for ZIF-8 versus **RHO** for ZIF-71). Evidenced by XRF and SEM-EDX mapping, ~10% of Zn(II) centers in ZIF-8 are exchanged by Mn(II) (Supporting Information, Table S1, Figures S7, S8). The EDX plot shows Kα signals of Mn and Zn in exchanged ZIF-8(Zn/Mn) with an average ratio of 0.117:1 (Mn:Zn), consistent with XRF data (0.135:1 Mn:Zn). Importantly, PXRD of exchanged ZIF-8(Zn/Mn) confirmed retention of **SOD** net (Supporting Information, Figure S9). A BET surface area of 1595 ± 116 $m^2/$

dx.doi.org/10.1021/ic400048g | Inorg. Chem. 2013, 52, 4011−4016

g was obtained for ZIF-8(Zn/Mn), compared with 1531 ± 99 m^2/g for pristine ZIF-8(Zn) (Supporting Information, Table S3). These results support metal cation exchange of the framework, as opposed to trapping of Mn(II) species in pores, which would be expected to reduce the available surface area.

The findings here complement recent work by Hupp and Cohen demonstrating PSE of the ligand components of ZIFs.[22−25] We sought to combine both forms of PSE in a stepwise fashion to consecutively exchange both metal ions and ligands. This process was explored in two different ways: (a) first exchange of the organic linker followed by exchange of the metal cation; and (b) the reverse process, exchange of the metal ion followed by organic ligand exchange.

4-Bromo-imidazole was chosen as the initial example for ligand exchange since ligand exchange can be readily monitored by SEM-EDX and ATOFMS (because of the Br atom), and no ZIFs have been reported based on this linker. Fully washed and activated ZIF-71(Zn) particles were incubated in a MeOH solution of 4-bromo-imidazole (Br-im) at 55 °C for 3 days. The ZIFs, before and after linker exchange, were digested and examined by ^{1}H NMR, revealing that ∼35% of Br-im had been incorporated into the ZIF (replacing the initial 4,5-dichlor-oimidazole,Cl_2-im, Supporting Information, Figure S12). EDX of exchanged ZIF-71(Cl_2/Br) exhibits signals of both Cl Kα (2.62 keV) and Br Lα (1.48 keV) (Supporting Information, Figure S13). This gives an average ratio of Br to Cl of 0.25:1, thus ∼33% Br-im incorporation, in agreement with the ^{1}H NMR. Ligand-based PSE was also evidenced by negative ion ATOFMS spectra, showing both Br (m/z = 79, 81) and Cl (m/z = 35, 37) ions in a single particle (Supporting Information, Figure S14). Thorough PSE was obtained, as essentially all of ∼1000 particles analyzed contained both halogens.

To examine the feasibility of stepwise PSE, exchanged ZIF-71(Cl_2/Br) was treated with Mn(acac)$_2$ in MeOH. PSE was successful, giving a bimetallic and multifunctional ZIF-71(Cl_2/Br)-(Zn/Mn). SEM-EDX mapping of stepwise-exchanged ZIF-71 exhibits a consistent and even distribution of Zn, Mn, Cl, and Br (Figure 2), confirming ∼12% Mn(II) metal

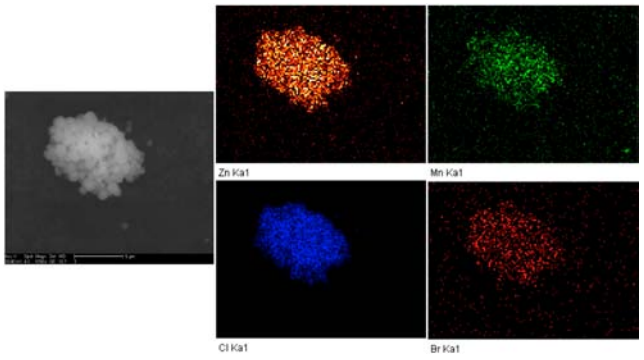

Figure 2. SEM-EDX mapping of exchanged ZIF-71(Cl_2/Br)-(Zn/Mn). SEM (left) and corresponding elemental distribution of Zn (top middle, orange), Mn (top right, green), Cl (bottom middle, blue), and Br (bottom right, red). Scale bar = 1 μm.

incorporation (Supporting Information, Table S1). The ligand exchange ratio (Br-im:Cl_2-im) was unchanged (by ^{1}H NMR and EDX, Supporting Information, Figure S12, S15), indicating the stability of ZIF-71(Cl_2/Br) for metal-based PSE. ATOFMS of an individual particle showed both Zn (m/z = 64, 66, 68) and Mn (m/z = 55) ions, and both Br (m/z = 79, 81) and Cl (m/z = 35, 37) ions, indicative of successful consecutive ligand- and metal-based PSE in each particle (Figure 3). Importantly,

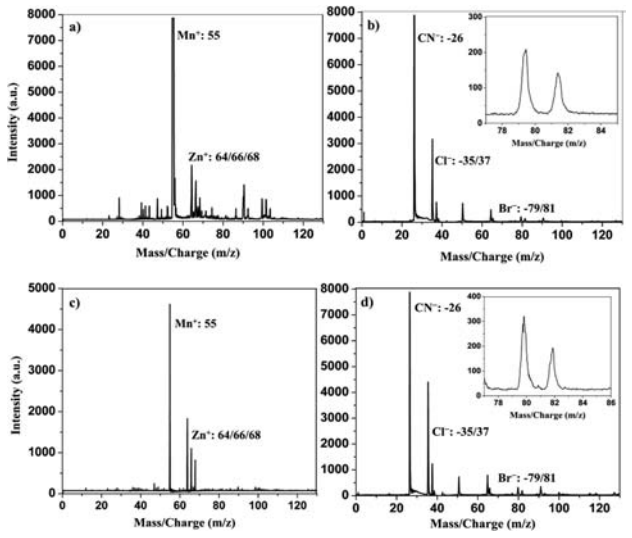

Figure 3. ATOFMS spectra for exchanged ZIF-71. Top: positive (a) and negative (b) ion spectra of ZIF-71(Cl_2/Br)-(Zn/Mn). Bottom: positive (c) and negative (d) ion spectra of exchanged ZIF-71(Zn/Mn)-(Cl_2/Br).

ATOFMS indicates that all of the microcrystalline particles (∼1000 particles analyzed) possess the desired multivariate ZIF-71(Cl_2/Br)-(Zn/Mn) composition. Retention of the zeotype **RHO** topology and crystallinity was verified by PXRD during the stepwise course of PSE (Figure 4).

Stepwise PSE on ZIF-71 via the reverse strategy was carried out with incubation of ZIF-71 with Mn(acac)$_2$ in MeOH for 1 day followed by Br-im in MeOH for 3 days (Scheme 2). Monitored by ^{1}H NMR and EDX, 30% of Br-im were incorporated into ZIF-71(Zn/Mn), replacing the initial Cl_2-im linker (Supporting Information, Figure S15 and S16). The ratio of metal ions remains essentially identical during ligand-based PSE (Supporting Information, Table S1). Metal ion PSE results in ZIF-71(Zn/Mn)-(Cl_2/Br), which contains ∼12% Mn(II) and retains 30% Br-im incorporation. Overall, the product is similar to the material obtained by reversing the order of the PSE processes (ZIF-71(Cl_2/Br)-(Zn/Mn)). SEM-EDX mappings of resultant postexchange solids suggest a consistent distribution of both exchanged ligands (Br vs Cl mapping) and metal ions (Mn vs Zn mapping) (Supporting Information, Figure S17). Again, ATOFMS indicate all of the particles undergo PSE with Mn, Zn, Cl, and Br ions found in the spectra of all particles (Figure 3).

To demonstrate the generality of PSE, ZIF-8 was also investigated for tandem metal ion and ligand PSE in both of the same fashions. 2-Ethyl-imidazole (eim) was employed for the exchanging ligand. Overall exchange yields of PSE were relatively low (∼10−20%), as determined by SEM-EDX for metal ion PSE and by ^{1}H NMR for ligand PSE (Supporting Information, Figures S18, S19, and S20). However, both strategies produce ZIF-8 with mixed metals and ligands (denoted ZIF-8(mim/eim)-(Zn/Mn)). After PSE, the materials remain crystalline and isoreticular to the parent ZIF-8(Zn) with **SOD** topology, as verified by PXRD (Figure 4).

dx.doi.org/10.1021/ic400048g | Inorg. Chem. 2013, 52, 4011−4016

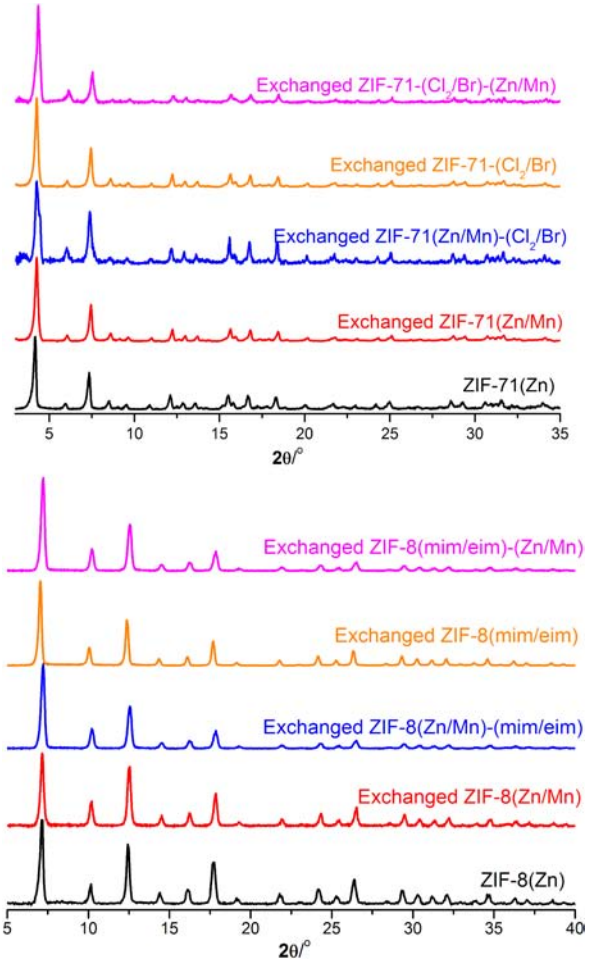

Figure 4. PXRD of ZIF-71 (top) and ZIF-8 (bottom) before and after metal ion and ligand PSE.

Scheme 2. Stepwise Metal Ion (Mn) and Ligand (Br-im) PSE of ZIF-71

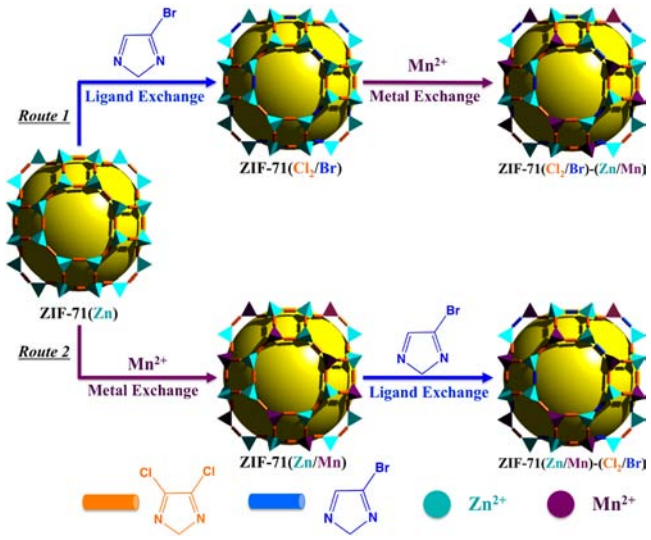

CONCLUSIONS

PSE is shown to be a general approach for introducing redox-active Mn(II) centers into "inert" ZIFs under ambient conditions. Postexchange materials are the first group of porous, Mn(II)-based ZIFs, which have been thoroughly characterized by several methods including ATOFMS. This demonstrates the utility of PSE to synthesize new materials that are unattainable by other currently available synthetic approaches. Consecutive cation and ligand exchange via biphasic (solid/liquid) PSE were successfully carried out for the first time in a "tandem" stepwise fashion. Monitored by ATOFMS and SEM-EDX, incoming metal ion and ligand were observed in a single exchanged ZIF particle, and essentially all particles undergo PSE. This study demonstrates the lability of metal−nitrogen bonding between metal centers and imidazolates, and thus dynamics of both inorganic and organic structural components in ZIFs.

ASSOCIATED CONTENT

Supporting Information

Further details are given in Tables S1−S3 and Figures S1−S20. This material is available free of charge via the Internet at http://pubs.acs.org.

AUTHOR INFORMATION

Corresponding Author

*E-mail: scohen@ucsd.edu.

Notes

The authors declare no competing financial interest.

ACKNOWLEDGMENTS

This work was supported by a grant from Department of Energy, Office of Basic Energy Sciences, Division of Materials Sciences and Engineering under Award No. DE-FG02-08ER46519.

REFERENCES

(1) O'Keeffe, M.; Yaghi, O. M. *Chem. Rev.* **2012**, *112*, 675.
(2) Sumida, K.; Rogow, D. L.; Mason, J. A.; McDonald, T. M.; Bloch, E. D.; Herm, Z. R.; Bae, T.-H.; Long, J. R. *Chem. Rev.* **2012**, *112*, 724.
(3) Li, J.-R.; Sculley, J.; Zhou, H.-C. *Chem. Rev.* **2012**, *112*, 869.
(4) Yoon, M.; Srirambalaji, R.; Kim, K. *Chem. Rev.* **2012**, *112*, 1196.
(5) Kreno, L. E.; Leong, K.; Farha, O. K.; Allendorf, M.; Van Duyne, R. P.; Hupp, J. T. *Chem. Rev.* **2012**, *112*, 1105.
(6) Eddaoudi, M.; Kim, J.; Rosi, N.; Vodak, D.; Wachter, J.; O'Keeffe, M.; Yaghi, O. M. *Science* **2002**, *295*, 469.
(7) Wang, Z.; Cohen, S. M. *Chem. Soc. Rev.* **2009**, *38*, 1315.
(8) Tanabe, K. K.; Cohen, S. M. *Chem. Soc. Rev.* **2011**, *40*, 498.
(9) Cohen, S. M. *Chem. Rev.* **2012**, *112*, 970.
(10) Tanabe, K. K.; Allen, C. A.; Cohen, S. M. *Angew. Chem., Int. Ed.* **2010**, *49*, 9730.
(11) Sato, H.; Matsuda, R.; Sugimoto, K.; Takata, M.; Kitagawa, S. *Nat. Mater.* **2010**, *9*, 661.
(12) Teppei, Y.; Kitagawa, H. *J. Am. Chem. Soc.* **2009**, *131*, 6312.
(13) Deshpande, R. K.; Minnaar, J. L.; Telfer, S. G. *Angew. Chem., Int. Ed.* **2010**, *49*, 4598.
(14) Das, S.; Kim, H.; Kim, K. *J. Am. Chem. Soc.* **2009**, *131*, 3814.
(15) Prasad, T. K.; Hong, D. H.; Suh, M. P. *Chem.—Eur. J.* **2010**, *16*, 14043.
(16) Zhang, Z.; Zhang, L.; Wojtas, L.; P., N.; Eddaoudi, M.; Zaworotko, M. J. *J. Am. Chem. Soc.* **2012**, *134*, 924.
(17) Brozek, C. K.; Dinca, M. *Chem. Sci.* **2012**, *3*, 2110.
(18) Burnett, B. J.; Barron, P. M.; Hu, C. H.; Choe, W. *J. Am. Chem. Soc.* **2011**, *133*, 9984.
(19) Lee, C. Y.; Farha, O. K.; Hong, B. J.; Sarjeant, A. A.; Nguyen, S. T.; Hupp, J. T. *J. Am. Chem. Soc.* **2011**, *133*, 15858.
(20) Demessence, A.; D'Alessandro, D. M.; Foo, M. L.; Long, J. R. *J. Am. Chem. Soc.* **2009**, *131*, 8784.
(21) Cychosz, K. A.; Matzger, A. J. *Langmuir* **2010**, *26*, 17198.

(22) Karagiaridi, O.; Lalonde, M. B.; Bury, W.; Sarjeant, A. A.; Farha, O. K.; Hupp, J. T. *J. Am. Chem. Soc.* **2012**, *134*, 18790.
(23) Kim, M.; Cahill, J. F.; Fei, H.; Prather, K. A.; Cohen, S. M. *J. Am. Chem. Soc.* **2012**, 18082.
(24) Kim, M.; Cahill, J. F.; Su, Y.; Prather, K. A.; Cohen, S. M. *Chem. Sci.* **2012**, *3*, 126.
(25) Karagiaridi, O.; Bury, W.; Sarjeant, A. A.; Stern, C. L.; Farha, O. K.; Hupp, J. T. *Chem. Sci.* **2012**, *3*, 3256.
(26) Cavka, J. H.; Jakobsen, S.; Olsbye, U.; Guillou, N.; Lamberti, C.; Bordiga, S.; Lillerud, K. P. *J. Am. Chem. Soc.* **2008**, *130*, 13850.
(27) Ferey, G.; Serre, C. *Chem. Soc. Rev.* **2009**, *38*, 1380.
(28) Phan, A.; Doonan, C. J.; Uribe-Romo, F. J.; Knobler, C. B.; O'Keeffe, M.; Yaghi, O. M. *Acc. Chem. Res.* **2009**, *43*, 58.
(29) Park, K. S.; Ni, Z.; Cote, A. P.; Choi, J. Y.; Huang, R.; Uribe-Romo, F. J.; Chae, H. K.; O'Keeffe, M.; Yaghi, O. M. *Proc. Natl. Acad. Sci. U.S.A.* **2006**, *103*, 10186.
(30) Zhang, J.-P.; Zhang, Y.-B.; Lin, J.-B.; Chen, X.-M. *Chem. Rev.* **2012**, *112*, 1001.
(31) Takaishi, S.; DeMarco, E. J.; Pellin, M. J.; Farha, O. K.; Hupp, J. T. *Chem. Sci.* **2012**, *4*, 1509−1513.
(32) Lively, R. P.; Dose, M. E.; Thompson, J. A.; McCool, B. A.; Chance, R. R.; Koros, W. J. *Chem. Commun.* **2011**, *47*, 8667.
(33) Venna, S. R.; Jasinski, J. B.; Carreon, M. A. *J. Am. Chem. Soc.* **2010**, *132*, 18030.
(34) Gard, E.; Mayer, J. E.; Morrical, B. D.; Dienes, T.; Fergenson, D. P.; Prather, K. A. *Anal. Chem.* **1997**, *69*, 4083.
(35) Kim, M.; Cahill, J. F.; Prather, K. A.; Cohen, S. M. *Chem. Commun.* **2011**, *47*, 7629.